www.elsevier.nl/locate/jorganchem

Journal of Organometallic Chemistry 619 (2001) 141–151

Journal of Organometallic Chemistry

The effect of different bithienyl spacers on the linear and non-linear optical properties of organometallic chromophores derived from $[Fe_2(\eta^5\text{-}C_5H_5)_2(CO)_2(\mu\text{-}CO)(\mu\text{-}C\text{–}CH_3)]^+$ $[BF_4]^-$ Crystal structure of $[Fe_2(\eta^5\text{-}C_5H_5)_2(CO)_2(\mu\text{-}CO)(\mu\text{-}(E)\text{-}C\text{–}CH{=}CH\text{-}7\text{-}(\text{thieno}[3,2\text{-}e][1]\text{benzothiophene})))]^+$ $[BF_4]^-$

Richard D.A. Hudson* [a,1], Anthony R. Manning* [a,2], David F. Nolan [a],
Inge Asselberghs [b], Roel Van Boxel [b], André Persoons [b], John F. Gallagher [c]

[a] *Department of Chemistry, University College Dublin, Belfield, Dublin 4, Ireland*
[b] *Katholieke Universiteit Leuven, Celestijnenlaan 200D, B-3001 Leuven, Belgium*
[c] *School of Chemical Sciences, Dublin City University, Dublin 9, Ireland*

Received 6 July 2000; accepted 3 August 2000

Abstract

Two series of organometallic merocyanines incorporating a variety of bithienyl moieties both as spacers and end groups were synthesised. In the first series the bithienyls function as end groups and were appended to an acceptor derived from $[Fe_2(\eta^5\text{-}C_5H_5)_2(CO)_2(\mu\text{-}CO)(\mu\text{-}C\text{–}CH_3)]^+$ $[BF_4]^-$. In the second series, ferrocene acting as an organometallic donor was incorporated into the chromophores at the far terminus of the bithienyl spacers. The molecular first hyperpolarisabilities β of the second series were determined by hyper-Rayleigh scattering and the values range from 429×10^{-30} esu to 867×10^{-30} esu in dichloromethane. A single crystal X-ray study of $[Fe_2(\eta^5\text{-}C_5H_5)_2(CO)_2(\mu\text{-}CO)(\mu\text{-}(E)\text{-}C\text{–}CH{=}CH\text{-}7\text{-}(\text{thieno}[3,2\text{-}e][1]\text{benzothiophene})))]^+$ $[BF_4]^-\cdot CH_2Cl_2$ is reported. © 2001 Elsevier Science B.V. All rights reserved.

Keywords: Non-linear optics; Hyper-Raleigh scattering; Hyperpolarisablity; Bithienyl; Iron; Ferrocene

1. Introduction

Organometallic moieties have been recognised recently as good candidates for the design of molecules exhibiting non-linear optical (NLO) properties [1]. The central metal atom of an organometallic complex can readily coordinate to conjugated ligands and undergo π-orbital overlap, facilitating effective charge transfer transitions leading to large dipole moment changes between the ground and excited states. Typically NLO compounds comprise donor and acceptor moieties bridged by a π-conjugated linker [2]. $[Fe_2(\eta^5\text{-}C_5H_5)_2(CO)_2(\mu\text{-}CO)(\mu\text{-}C\text{–}CH_3)]^+$ $[BF_4]^-$ [**1**]BF_4 (Fig. 1), originally synthesised by Rosenblum [3], was identified by Green and co-workers [4] as a good acceptor candidate since the μ-alkylidyne carbon atom has a formally vacant perpendicular p-orbital which can accept electron density from a vinyl group throughout rotation about the μC-C(vinyl) bond [5]. As the cationic diiron moiety can be extended by vinyl groups through facile condensation of [**1**]BF_4 with aldehydes [6], Green and co-workers were able to synthesise a small number of derivatives of [**1**]BF_4 and study their NLO responses with promising results. Our group has had an interest in the iron dimer $Fe_2(\eta^5\text{-}C_5H_5)_2(CO)_4$ and related compounds for a number of years and has recently sought to extend [7] the pioneering work of Green [4] with the aim of synthesising more organometallic compounds with NLO properties.

---

[1] *Corresponding author. E-mail address: richard.hudson@ucd.ie.

[2] Corresponding author. Tel.: +353-1-716-2311; fax: +353-1-716-2127; e-mail: anthony.manning@ucd.ie.

PII: S0022-328X(00)00569-6

2. Results and discussion

In order to achieve the best NLO response from a system it is necessary to identify a combination of well matched elements. A survey of the literature of donor–π-acceptor (DπA) compounds and conducting organic polymers highlights the utility of the thienyl residue as an efficient and readily available relay for electronic transmission [8]. Having picked [**1**]BF$_4$ (Fig. 1) as our acceptor we chose a number of bithienyl compounds (**a**–**e**) [9–13] (Fig. 2) to complete the chromophores, allowing us to vary the length of the conjugated linker and to investigate differing degrees of rigidity and aromaticity.

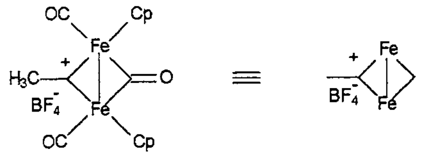

[**1**]BF$_4$ [**1**]BF$_4$

Fig. 1. [**1**]BF$_4$ ([Fe$_2$(η^5-C$_5$H$_5$)$_2$(CO)$_2$(μ-CO)(μ-C–CH$_3$)]$^+$ [BF$_4$]$^-$).

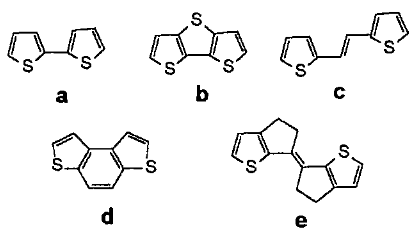

Fig. 2. Bithienyl spacers **a**–**e**.

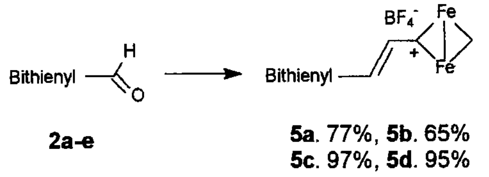

Scheme 1. Reagents and conditions: [**1**]BF$_4$, CH$_2$Cl$_2$, reflux 18 h.

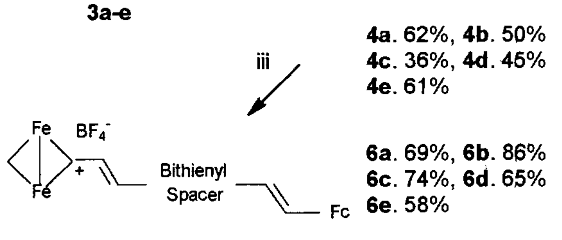

Scheme 2. Reagents and conditions: i, [FcCH$_2$PPh$_3$]I, KOH aq., CH$_2$Cl$_2$, 1 h; ii, I$_2$ cat., CH$_2$Cl$_2$, reflux, 1 h; iii, [**1**]BF$_4$, CH$_2$Cl$_2$, reflux 18 h.

Thus, bithiophene **a** [9] was rigidified by the inclusion of a sulfur bridge to form **b** [10] or extended by a vinylic spacer to afford **c** [11]. Rigidification of **c** was effected by photocyclisation to form **d** [12] or by configurationally locking the central double bond to give **e** [13]; both strategies force the thiophenes to adopt a coplanar arrangement. Roncali has compared poly(**c**) and poly(**e**) and concluded that there is a considerable reduction in band gap on restriction of interannular rotations around the single bonds of the oligomers [13]. It was anticipated that this lengthening and rigidification leading to improved π-orbital overlap would afford a more efficient π-conjugated spacer and consequently better NLO chromophores. We describe here the synthesis and properties of the series of chromophores [**5a**–**5e**]BF$_4$ and [**6a**–**6e**]BF$_4$.

2.1. Synthesis of [5a–5e]BF$_4$ and [6a–6e]BF$_4$

Established procedures were used to convert the thiophene derivatives **a**–**e** to monoaldehydes **2** [14] and dialdehydes **3** [15]. The ferrocene aldehydes **4** were prepared from **3** by Wittig reactions with FcCH$_2$PPh$_3$I [16] and were all formed as configurational isomers in a *Z*:*E* ratio of approximately 2:3. Isomerisation with iodine in refluxing dichloromethane cleanly afforded the required all-*trans* materials which are red air-stable solids, soluble in normal organic solvents.

The aldehydes **2** and **4** were condensed with **1** to afford the cationic merocyanines [**1**]BF$_4$, (Scheme 1) and [**6**]BF$_4$ (Scheme 2). Purification by precipitation of dichloromethane solutions of the salts from diethyl ether gave the materials as highly coloured dark red to dark blue solids in good to excellent yields. These compounds are all soluble in polar organic solvents to give solutions which are reasonably air stable in the absence of light. Only [**5d**]BF$_4$ afforded single crystals suitable for X-ray analysis (Fig. 5). All the compounds exhibited the expected NMR and IR spectral data and analysed for between 0.25 and 1.0 mol of dichloromethane. This could not be removed under high vacuum and can clearly be seen in the ^{1}H-NMR spectra and is present as solvent of crystallisation in the crystal structure of [**5d**]BF$_4$. π-Excessive heteroaromatics are known to act as donors [17] and in [**5**]BF$_4$, the thienyls **a**–**e** act as donating end groups albeit complex ones, whilst in [**6**]BF$_4$ they are part of the spacer between the Fe$_2$(η^5-C$_5$H$_5$)$_2$(CO)$_2$(CO)(μ-C–)$^+$ acceptor and the ferrocene donor of the merocyanine.

2.2. NMR and linear optical properties

2.2.1. Infrared and NMR spectra

The IR and ^{13}C-NMR spectroscopic details for the carbonyl stretching frequencies and the μ-carbon chemical shift values (ppm) for compounds [**5**]BF$_4$ and

Table 1
Infrared (CO region) and ^{13}C-NMR (μ-carbyne) spectroscopic data for [**5**]BF$_4$ and [**6**]BF$_4$

No.	IR-bands (cm^{-1}) [a]	^{13}C-NMR δ (ppm) [b]	No.	IR-bands (cm^{-1}) [a]	^{13}C-NMR δ (ppm) [b]
1	2046, 2012, 1853	499 [c]	**1**	2046, 2012, 1853	499 [c]
5a	2033, 2005, 1842	418.8	**6a**	2031, 1996, 1842	412.5
5b	2033, 1995, 1841	n/a	**6b**	2031, 2000, 1841	409.6
5c	2031, 2002, 1842	415.8	**6c**	2030, 2001, 1839	411.5
5d	2035, 2006, 1842	428.2	**6d**	2036, 2006, 1844	426.8
5e	2024, 1995, 1834	394.1	**6e**	2032, 1995, 1833	385.3

[a] Recorded in dichloromethane.
[b] ^{13}C-NMR spectra recorded in d_2-dichloromethane.
[c] Recorded in d-chloroform.

[**6**]BF$_4$ are recorded in Table 1. The IR absorbances in the ν(CO) region are considerably shifted from the values for [**1**]BF$_4$ reflecting the greater degree of delocalisation of the positive charge away from the μ-carbon onto the organic ligand. The values change in the order $[\mathbf{5}(\mathbf{d}>\mathbf{a}>\mathbf{b}>\mathbf{c}>\mathbf{e})]\mathrm{BF}_4$ and $[\mathbf{6}(\mathbf{d}>\mathbf{a}>\mathbf{b}>\mathbf{c}>\mathbf{e})]\mathrm{BF}_4$, but the extremes corresponding to **d** and **e** in both series [**5**]BF$_4$ and [**6**]BF$_4$ are not particularly marked. However, the trends in the ^{13}C-NMR chemical shifts are much more obvious. The extremely low field peak at δ 499 in [**1**]BF$_4$, corresponding to the bridging carbyne carbon, is considerably shifted upfield for [**5**]BF$_4$ and [**6**]BF$_4$, demonstrating the increase in electron density on the μ-carbon along the series $[\mathbf{5}(\mathbf{d}<\mathbf{a}<\mathbf{c}<\mathbf{e})]\mathrm{BF}_4$ and $[\mathbf{6}(\mathbf{d}<\mathbf{a}<\mathbf{b}<\mathbf{c}<\mathbf{e})]\mathrm{BF}_4$. The ^{1}H-NMR spectra often show considerable broadening in the μC–C*H*=C*H* region (possibly due to slowed rotation with increasing delocalisation across the series) and so the coupling constants across the double bond adjacent to the diiron moiety cannot always be ascertained. In those circumstances where they could, the J values are all 13.7 Hz (with the exception of [**5b**]BF$_4$ at 12.7 Hz) suggesting an E-configuration and this was confirmed in the case of [**5d**]BF$_4$ by X-ray analysis. For compounds [**5c**]BF$_4$ and [**6c**]BF$_4$ there is a double bond between the thiophene residues with J_{HH} coupling constants of 16.1 and 15.6 Hz, respectively. Compounds [**6**]BF$_4$ have a further double bond adjacent to the ferrocene and this has a coupling constant of ca. 16 Hz in all cases (for compound [**6d**]BF$_4$ the vinyl protons in this region are coincident and so no coupling constant is observed). This increase in coupling constant with distance from the iron cluster is consistent with an increase in bond order. Indeed the reduced bond length alternation next to the acceptor may be seen clearly in the X-ray structure for [**5d**]BF$_4$ (Fig. 5). Unfortunately, the ^{1}H-NMR spectrum for [**6e**]BF$_4$, the most promising of our NLO candidates, was so broadened that no fine structure could be seen at all even after several filtrations and attempts at purification by reprecipitation.

2.2.2. UV–Vis spectra

It is widely recognised that low energy bands in the UV–Vis spectra [18] and large solvatochromism [19] are good indicators of potential NLO properties. The UV–Vis spectra of [**5**]BF$_4$ and [**6**]BF$_4$ recorded in dichloromethane (1×10^{-5} M) are shown in Figs. 3 and 4 and summarised along with the data recorded in acetonitrile in Table 2.

Compounds [**5**]BF$_4$ have one low energy band in the range 500–700 nm and we have characterised this as π–π* or ligand to metal charge transfer (LMCT) band for the thiophene-containing portion of the molecule. This band shifts to lower energies in the order $[\mathbf{5}(\mathbf{d}>\mathbf{a}>\mathbf{b}>\mathbf{c}>\mathbf{e})]\mathrm{BF}_4$ and exhibits large negative solvatochromism. The ferrocenyl derivatives [**6**]BF$_4$ have two bands in this region and, based on the work of Sarkar

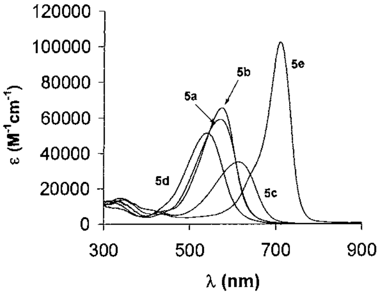

Fig. 3. UV–Vis absorption spectra for compounds [**5**]BF$_4$ recorded in CH$_2$Cl$_2$ at approx. 1×10^{-5} M concentration.

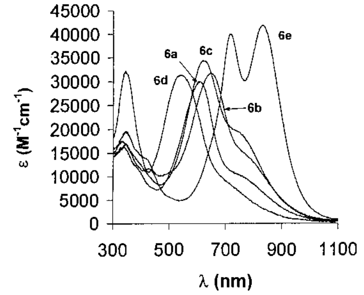

Fig. 4. UV–Vis absorption spectra for compounds [**6**]BF$_4$ recorded in CH$_2$Cl$_2$ at approx. 1×10^{-5} M concentration.

[20], we have characterised the higher energy peak as the π–π*/LMCT band and the band at longer wavelength as the metal to ligand CT (MLCT) band centred on ferrocene. Acetonitrile solutions of compounds [**6**]BF_4 exhibited the lower energy band as a shoulder and its position and intensity were estimated from the spectra. The position of this band could not be ascertained for compound [**6d**]BF_4 measured in acetonitrile as it is obscured by the much more intense π–π*/LMCT band. The position and intensity of both LMCT and MLCT bands follow the trend [**6**(**d** > **a** > **b** > **c** > **e**)]BF_4 and also exhibit a solvent dependence. It is noteworthy that as the conjugated linker becomes more effective along the series so the MLCT band becomes more intense relative to the π–π*/LMCT band reflecting the lower band gap and consequently more accessible first excited state in the order **d** > **a** > **b** > **c** > **e**.

*2.2.3. X-ray structure of [**5d**]BF_4*

An ORTEX [21] diagram of the molecular structure of compound [**5d**]BF_4 is presented in Fig. 5 together with selected bond lengths and angles. The structure shows that there is a considerable reduction in bond length alternation (BLA) adjacent to the diiron moiety. It has been shown [22] that the polarisabilities of linear polymethine dyes can be correlated with BLA and the closely related parameter, π-bond order alternation and so it is of interest to consider the π-system in these terms. The single bonds C(1)–C(2) 1.416(7) Å and C(3R)–C(4R) 1.419(7) Å are similar and shortened from the normal sp^2–sp^2 single bond length (1.48 Å) [23]. Similarly the double bond C(2)–C(3R) 1.362(7) Å is lengthened in comparison with a normal $sp^2{=}sp^2$ double bond (1.32 Å) [23]. The ligand lies in a slightly twisted arrangement with respect to the plane defined by the two iron atoms and the μ-carbon [dihedral angles Fe(1)–C(1)–C(2)–C(3R) = 161.8(5)°; Fe(2)–C(1)–C(2)–C(3R) = −23.6(10)°; C(1)–C(2)–C(3R)–C(4R) = −178.8(5)°; C(2)–C(3R)–C(4R)–C(5R) = 171.3(6)°] and is essentially planar. The bond lengths and angles within the fused ring system and the diiron system are not altered appreciably from the expected values. These observations are in accordance with the structure reported by Green [3] for the analogous compound in which [**1**]BF_4 was appended with a *p*-dimethylaminophenyl moiety and suggest that contributions from canonical forms in which the charge is delocalised into the adjacent π-system are important.

2.3. Non-linear optical properties

The HRS technique [24] was used to obtain the hyperpolarisability (*β*) of compounds [**6**]BF_4 using the external reference method and the results are sum-

Table 2
UV–Vis (π–π*/LMCT and MLCT) absorption data [a] and hyperpolarisability values for compounds [**5**]BF_4 and [**6**]BF_4

No.	λ_{max} (nm) (ε) [b] CH_3CN π–π*	λ_{max} (nm) (ε) [c] CH_2Cl_2 π–π*	No.	λ_{max} (nm) (ε) [d] CH_3CN π–π*	λ_{max} (nm) (ε) [d] CH_2Cl_2 π–π*	λ_{max} (nm) (ε) [d] CH_3CN MLCT	λ_{max} (nm) (ε) [d] CH_2Cl_2 MLCT	β [f] (10^{30}esu)	β_0 [f] (10^{30}esu)
[**5a**]BF_4	536 (43700)	568 (57150)	[**6a**]BF_4	577 (31650)	606 (27400)	670 [e] (15600)	733 (10500)	429	202
[**5b**]BF_4	545 (51250)	572 (65650)	[**6b**]BF_4	591 (36050)	621 (34350)	680 [e] (23400)	747 (19400)	624	307
[**5c**]BF_4	575 (44750)	612 (36300)	[**6c**]BF_4	648 (37350)	669 (37750)	680 [e] (35350)	750 (31200)	867	430
[**5d**]BF_4	509 (46000)	538 (51550)	[**6d**]BF_4	508 (29500)	543 (35200)	n/a	712 [e] (10600)	625	273
[**5e**]BF_4	680 (75900)	709 (105550)	[**6e**]BF_4	700 (37800)	716 (40100)	769 (40900)	830 (41850)	1243 [g]	697 [g]

[a] Molar concentrations were all approximately 1×10^{-5}.
[b] Recorded in dichloromethane.
[c] Recorded in d_2-dichloromethane.
[d] Units M^{-1} cm^{-1}.
[e] Estimated from spectra.
[f] Recorded at 1064 nm in dichloromethane ($\beta_{PNA} = 21.6\times10^{-30}$ esu).
[g] Fluorescence contribution.

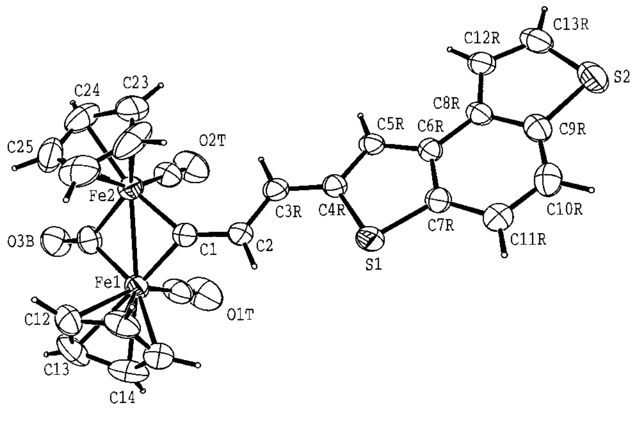

Fig. 5. ORTEX diagram of the organometallic cation [**5d**]BF_4 with the non-H atoms depicted with 30% probability ellipsoids. Selected bond lengths (Å): Fe(1)–Fe(2) = 2.5081(13); Fe(1)–C(1) = 1.831(5); Fe(2)–C(1) = 1.836(6); C(1)–C(2) = 1.416(7); C(2)–C(3R) = 1.362(7); C(3R)–C(4R) = 1.419(7). Selected bond angles (°): Fe(1)–C(1)–Fe(2) = 86.3(2); C(1)–Fe(1)–Fe(2) = 46.92(18); C(1)–Fe(2)–Fe(1) = 46.76(17); Fe(1)–C(1)–C(2) = 134.9(4); Fe(2)–C(1)–C(2) = 138.6(4); C(1)–C(2)–C(3R) = 124.2(6); C(2)–C(3R)–C(4R) = 126.4(6).

marised in Table 2. Fluorescence checks were made on all the compounds and only [**6e**]BF_4 was found to exhibit fluorescence which obscures the true hyperpolarisability. Although the 'two-level' model [25] is not strictly applicable in this case, it was used to calculate the static hyperpolarisabilities (β_0) and one should not take these values as absolute numbers. Nevertheless, the hyperpolarisabilities follow essentially the same trend encountered in the other spectroscopic measurements, increasing in the order [**6**(**a** < **b** ~ **d** < **c** < **e**]BF_4 whilst the static hyperpolarisabilities increase in the order [**6**(**a** < **d** < **b** < **c** < **e**)]BF_4. The apparent anomaly for compound [**6e**]BF_4 is due to resonance enhancement at the second harmonic wavelength.

The largest reported β value for an organometallic compound was for a zinc porphyrin complex [26]. However, β values for organometallic chromophores are generally in the range of 50×10^{-30}–700×10^{-30} esu [27] and our complexes fall at the upper end of this range. Indeed the values found for the ferrocenyl complexes [**6**]BF_4 are among the highest reported for this donor moiety.

3. Conclusions

π-Excessive heteroaromatics may act as good donors in their own right [17] and this is amply demonstrated by the spectroscopic differences between [**1**]BF_4 and [**5**]BF_4. The trends seen in the spectra for compounds [**5**]BF_4 show that rigidifying the systems must lead to increased orbital overlap and therefore to more effective electron delocalisation throughout the molecule. When the thiophene derivative acts as the linker within the merocyanine [**6**]BF_4 then the results clearly show that increasing the length of the linker ([**6a**]BF_4 and [**6c**]BF_4) and rigidification of the system ([**6a**]BF_4 and [**6b**]BF_4), alters the degree of communication between the donor and acceptor. However, introduction of the benzenoid motif into the system in order to rigidify the framework causes a barrier to charge transfer relative to the other structures as a consequence of the higher resonance energy of benzene relative to thiophene (36 and 25 kcal mol^{-1}, respectively) [28]. Measurement of the β values shows that there is a marked effect due to the nature of the spacer in this series. The values range from 429×10^{-30} esu for [**6a**]BF_4 to the much higher value of 867×10^{-30} esu for [**6c**]BF_4 excluding the fluorescence enhanced value of 1243×10^{-30} esu for [**6e**]BF_4. This demonstrates that tuning the non-linear optical response is possible by structural modification of the spacer. The initial study [4] of derivatives of [**1**]BF_4 for NLO response involved measurements by the Kurtz powder technique and revealed only small SHG efficiencies. This was attributed to unfavourable alignment of the chromophores in the centrosymmetric crystal lattice. The fact that any second harmonic signal at all was observed (0.77 and 3.6 times that of urea for $[Fe_2(\eta^5\text{-}C_5H_5)_2(CO)_2(\mu\text{-}CO)(\mu\text{-}C\text{–}(E)\text{–}CH{=}CHC_6H_4\text{-}4\text{-}NMe_2)]^+$ as the $[BF_4]^-$ and $[CF_3SO_3]^-$ salts respectively) suggested that derivatives of [**1**]BF_4 should have very large molecular second-order hyperpolarisabilities. Our measurements by the HRS method in solution have both avoided the problems associated with symmetry in the bulk state and validated the choice of [**1**]BF_4 as a good acceptor group.

We are currently investigating ways in which a cyclisation stategy can lock the system into a more extended coplanar arrangement by arresting the rotation of the bridging element at its junction with the metallocene donor.

4. Experimental

4.1. General methods

All reactions were performed under a nitrogen atmosphere. Diethyl ether and THF were freshly distilled from sodium benzophenone ketyl and toluene was distilled from sodium metal. $[Fe_2(\eta^5\text{-}C_5H_5)_2(CO)_2(\mu\text{-}CO)(\mu\text{-}C\text{–}CH_3)]^+$ $[BF_4]^-$ ([**1**]BF_4) was prepared according to the literature procedure [3]. All other chemicals and reagents were used as received without further purification. ^1H-NMR spectra were obtained on a Jeol 270 MHz spectrometer or Varian INOVA-500 MHz spectrometer. ^{13}C-NMR spectra were obtained on a Jeol 270 MHz spectrometer or Varian INOVA-500 MHz spectrometer operating at 68 and 126 MHz, respectively. FT-IR spectra were obtained on a Perkin–Elmer Paragon 1000 as either a solution in dichloromethane (windows: KBr, path length 0.1 mm) or in a KBr pellet. Relative peak heights are shown in parentheses. UV–Vis spectra were obtained on a UnicamUV2 spectrometer.

*4.2. General procedure for the Wittig condensation of **3a**–**3e** with (ferrocenylmethyl)triphenylphosphonium iodide [16] to afford **4a**–**4e***

(Ferrocenylmethyl)triphenylphosphonium iodide [16] (0.9 equivalent) and the required dialdehyde (1 equivalent) were stirred with a saturated aqueous solution of sodium hydroxide (50 equivalents) in dichloromethane (30 ml) at room temperature for 4 h. Analysis of the reaction mixture by TLC (CH_2Cl_2) indicated that the reaction was complete by the disappearance of the dialdehyde and the appearance of a faster eluting red band. The mixture was washed with several aliquots of water and the organic portion was dried over $MgSO_4$ before being evaporated to dryness in vacuo. The residue was separated by column chromatography on silica gel with dichloromethane–petroleum ether (1:1) followed by dichloromethane to elute the required compounds **4** as a mixture of isomers in the ratio 2:3 (*Z*:*E*). Isomerisation of the isomeric mixtures was carried by the action of a catalytic amount of iodine in refluxing dichloromethane (20 ml) for 1 h.

*4.2.1. 5-((E)-2-Ferrocenylethenyl)-2-thienyl)thiophene-2-carbaldehyde (**4a**)*

Experimental procedures and work-up were as described in Section 4.2. Experimental details: (ferrocenylmethyl)triphenylphosphonium iodide (0.232 g, 0.48 mmol), **3a** (0.096 g, 0.43 mmol). Yield: 0.121 g, 62% based on phosphonium salt. Obtained as a red crystalline solid. M.p. 212–214°C. ^{1}H-NMR (500 MHz, $CDCl_3$): δ 9.78 (s, 1H, C*H*O), 7.59 (d, 1H, *J* 4.0 Hz, Th), 7.15 (m, 2H, Th), 6.82 (d, 1H, *J* 3.8 Hz, Th), 6.69 (s, 2H, Fc–C*H*=C*H*), 4.38 (m, 2H, Fcα*H*), 4.26 (m, 2H, Fcβ*H*), 4.09 (s, 5H, C_5H_5). ^{13}C-NMR (126 MHz, $CDCl_3$): δ 182.7, 147.8, 145.9, 141.5, 137.9, 133.3, 129.5, 127.2, 125.8, 123.9, 118.8, 82.5, 69.9, 69.6, 67.3. IR (CH_2Cl_2): 1662(10), 1622(1), 1472(1.5), 1383(1), 1223(2), 1047(1.5) cm^{-1}. Anal. Calc. for $C_{21}H_{16}OS_2 \cdot 0.5H_2O$: C, 61.02; H, 4.12. Found: C, 61.15; H, 3.87%. UV–Vis (CH_2Cl_2): λ_{max} 418 nm.

*4.2.2. 6-((E)-2-Ferrocenylethenyl)dithieno[3,2-b:2,3-d]-thiophene-3-carbaldehyde (**4b**)*

Experimental procedures and work-up were as described in Section 4.2. Experimental details: (ferrocenylmethyl)triphenylphosphonium iodide (0.483 g, 1.0 mmol), **3b** (0.270 g, 1.07 mmol). Yield: 0.217 g, 50% based on phosphonium salt. Obtained as a red solid. M.p. > 260°C (dec.). ^{1}H-NMR (270 MHz, $CDCl_3$): δ 9.88 (s, 1H, C*H*O), 7.86 (1H, s, Th), 7.08 (s, 1H, Th), 6.78 (s, 2H, Fc–C*H*=C*H*), 4.42 (m, 2H, Fcα*H*), 4.29 (m, 2H, Fcβ*H*), 4.10 (s, 5H, C_5H_5). [1.53, (H_2O)]. IR (CH_2Cl_2): 1662(10), 1620(2), 1492(4), 1384(1.5), 1372(1.5), 1227(3), 1140(3) cm^{-1}. Anal. Calc. for $C_{21}H_{14}FeOS_3 \cdot H_2O$: C, 55.75; H, 3.54. Found: C, 55.40; H, 3.16%. UV–Vis (CH_2Cl_2): λ_{max} 415 nm.

*4.2.3. 5-((E)-2-(5-((E)-2-Ferrocenylethenyl)-2-thienyl)ethenyl)thiophene-3-carbaldehyde (**4c**)*

Experimental procedures and work-up were as described in Section 4.2. Experimental details: (ferrocenylmethyl)triphenylphosphonium iodide (0.483 g, 1.0 mmol), **3c** (0.270 g, 1.09 mmol). Yield: 0.080 g, 36% based on phosphonium salt. Obtained as a red solid. M.p. > 250°C (dec.). ^{1}H-NMR (270 MHz, $CDCl_3$): δ 9.84 (s, 1H, C*H*O), 7.65 (d, 1H, *J* 4.0 Hz, Th), 7.21 (d, 1H, *J* 15.8 Hz, OHC–Th–C*H*=CH–Th), 7.10 (d, 1H, *J* 4.0 Hz, Th), 6.99 (d, 1H, *J* 3.7 Hz, Th), 6.96 (d, 1H, *J* 15.8 Hz, Th–CH=C*H*–Th), 6.85 (d, 1H, *J* 3.7 Hz, Th), 6.76 (d, 1H, *J* 15.8 Hz, Fc–C*H*=CH), 6.73 (d, 1H, *J* 15.8 Hz, Fc–CH=C*H*), 4.41 (m, 2H, Fcα*H*), 4.32 (m, 2H, Fcβ*H*), 4.16 (s, 5H, C_5H_5), [1.55, (H_2O)]. ^{13}C-NMR (68 MHz, $CDCl_3$): δ 182.7, 152.6, 144.8, 141.5, 139.3, 137.7, 129.8, 129.1, 126.6, 126.2, 125.9, 119.9, 119.5, 83.4, 70.0, 69.9, 67.3. IR (CH_2Cl_2): 1660(10), 1602(3), 1514(1), 1445(4), 1365(1), 1226(6), 1048(3), 942(2) cm^{-1}. Anal. Calc. for $C_{23}H_{18}FeOS_2 \cdot 0.5H_2O$: C, 62.87; H, 4.33. Found: C, 62.60; H, 4.28%. UV–Vis (CH_2Cl_2): λ_{max} 432 nm.

*4.2.4. 7-((E)-2-Ferrocenylethenyl)thieno[3,2-e][1]-benzothiophene-2-carbaldehyde (**4d**)*

Experimental procedures and work-up were as described in Section 4.2. Experimental details: (ferrocenylmethyl)triphenylphosphonium iodide (0.386 g, 0.8 mmol), **3d** (0.221 g, 0.9 mmol). Yield: 0.141 g, 45% based on phosphonium salt. Obtained as a red solid. ^{1}H-NMR (500 MHz, $CDCl_3$): δ 10.15 (s, 1H, C*H*O), 8.30 (s, 1H, Th), 7.84 (d, 1H, *J* 8.8 Hz, C_6H_2), 7.74 (d, 1H, *J* 8.8 Hz, C_6H_2), 7.53 (1H, s, Th), 6.96 (d, 1H, *J* 15.6 Hz, Fc–C*H*=CH), 6.89 (d, 1H, *J* 15.6 Hz, Fc–CH=C*H*), 4.52 (m, 2H, Fcα*H*), 4.37 (m, 2H, Fcβ*H*), 4.19 (s, 5H, C_5H_5), [1.59, (H_2O)]. ^{13}C-NMR (126 MHz, $CDCl_3$): δ 184.6, 146.3, 143.2, 141.0, 137.2, 135.7, 133.5, 132.1, 131.4, 122.9, 119.3, 119.0, 118.9, 82.3, 70.0, 69.7, 67.5. IR (CH_2Cl_2): 1672(10), 1623(1), 1606(1), 1576(1), 1500(1.5), 1336(2), 1132(3), 1106(1) cm^{-1}. Anal. Calc. for $C_{23}H_{16}FeOS_2$: C, 46.48; H, 3.74. Found: C, 46.26; H, 3.49%. UV–Vis (CH_2Cl_2): λ_{max} 358 nm.

*4.2.5. 2′-((E)-2-Ferrocenylethenyl)-4,5,4′,5′-tetrahydro-[6,6′]bi[cyclopenta[b]thiophenylidene]-2-carbaldehyde (**4e**)*

Experimental procedures and work-up were as described in Section 4.2. Experimental details: (ferrocenylmethyl)triphenylphosphonium iodide (0.290 g, 0.6 mmol), **3e** (0.200 g, 0.67 mmol). Yield: 0.197 g, 61% based on phosphonium salt. Obtained as a red solid. M.p. > 300°C (dec.). ^{1}H-NMR (270 MHz, $CDCl_3$): δ 9.78 (s, 1H, C*H*O), 7.52 (s, 1H, Th), 6.78 (s, 1H, Th), 6.73 (s, 2H, Fc–C*H*=C*H*), 4.46 (m, 2H, Fcα*H*), 4.33 (m, 2H, Fcβ*H*), 4.17 (s, 5H, C_5H_5), 3.33 (m, 2H, CH_2), 3.21 (m, 2H, CH_2), 3.05 (m, 4H, CH_2,CH_2), [1.58, (H_2O)]. ^{13}C-NMR (75 MHz, $CDCl_3$): δ 182.6, 154.6, 154.1, 151.1, 150.4, 146.8, 141.4, 133.8, 132.2, 127.5, 125.5, 121.0, 120.2, 83.3, 69.8, 69.7, 67.1, 35.5, 34.8, 27.9, 27.1. IR (CH_2Cl_2): 1652(10), 1607(9.5), 1516(1), 1400(5), 1341(1.5), 1135(4) cm^{-1}. Anal. Calc. for $C_{27}H_{22}FeOS_2{\cdot}H_2O$: C, 64.80; H, 4.80. Found: C, 64.86; H, 4.64%. UV–Vis (CH_2Cl_2): λ_{max} 470 nm.

*4.3. General procedure for the condensation of $[Fe_2(\eta^5\text{-}C_5H_5)_2(CO)_2(\mu\text{-}CO)(\mu\text{-}C\text{–}CH_3)]^+$ $[BF_4]^-$ ([**1**]BF_4) with **2a**–**2e** and **4a**–**4e** to afford [**5a**–**5e**]BF_4 and [**6a**–**6e**]BF_4*

Following the procedure of Casey [6], ([**1**]BF_4) (1 equivalent) and the required aldehyde (2 equivalents) were stirred at reflux in dichloromethane (5–10 ml). The reactions were monitored by IR spectroscopy for the disappearance of the ν_{CO} bands of the starting material which took approximately 18 h. The volume of the solvent was reduced in vacuo to half the original amount and the product was isolated by precipitation by the addition of diethyl ether (50–100 ml). The precipitate was collected by filtration and redissolved in a minimum volume of dichloromethane before being re-precipitated by the addition of diethyl ether (100 ml). This was repeated and the solid was dried under high vacuum.

*4.3.1. $[Fe_2(\eta^5\text{-}C_5H_5)_2(CO)_2(\mu\text{-}CO)(\mu\text{-}(E)\text{-}C\text{–}CH{=}CH\text{-}2\text{-}(5\text{-}thienyl)thiophene))]^+$ $[BF_4]^-$ (**5a**)*

Experimental procedures and work-up were as described in Section 4.3. Experimental details: **2a** (0.130 g, 0.7 mmol), [**1**]BF_4 (0.130 g, 0.3 mmol). Yield: 0.142 g, 77% based on [**1**]BF_4. Obtained as a dark purple solid. M.p. > 210°C (dec.). ^{1}H-NMR (500 MHz, CD_2Cl_2): δ 9.39 (bs, 1H, μ-C–C*H*), 8.20 (bs, 1H, Th), 7.91 (bs, 1H, μ-C–CH=C*H*), 7.48 (bs, 1H, Th), 7.45 (d, 1H, *J* 4.9 Hz, Th), 7.36 (bs, 1H, Th), 7.10 (bs, 1H, Th), 5.23 (s, 10H, C_5H_5). ^{13}C-NMR (126 MHz, CD_2Cl_2): δ 418.8 (μ-*C*), 255.0 (μ-*C*O), 207.9 (*C*O), 153.3, 150.4, 146.7, 146.1, 138.7, 136.8, 130.3, 130.0, 128.9, 128.5, 92.3. IR (CH_2Cl_2): 2033(^{t}CO, 10), 2005 (^{t}CO, 2.5), 1842 (μ-CO, 5), 1605(2), 1542(5), 1516(10), 1378(3), 1343(2.5), 1187(10), 1149(4), 1052(5) cm^{-1}. IR (KBr disc): 2012 (^{t}CO, 7), 1979 (^{t}CO, 5), 1828 (μ-CO, 5), 1636(7), 1539(6), 1513(10), 1439(5), 1374(3), 1185(5), 1147(4) cm^{-1}. Anal. Calc. for $C_{24}H_{17}BF_4Fe_2O_3S_2{\cdot}0.5CH_2Cl_2$: C, 44.64; H, 2.73. Found: C, 44.97; H, 2.72%. UV–Vis (CH_3CN): λ_{max} (ε) 536 (43700 M^{-1} cm^{-1}), 330 nm (14950 M^{-1} cm^{-1}). UV–Vis (CH_2Cl_2): λ_{max} (ε) 568 (57150 M^{-1} cm^{-1}), 315 nm (13050 M^{-1} cm^{-1}).

*4.3.2. $[Fe_2(\eta^5\text{-}C_5H_5)_2(CO)_2(\mu\text{-}CO)(\mu\text{-}(E)\text{-}C\text{–}CH{=}CH\text{-}2\text{-}(6\text{-}dithieno[3,2\text{-}b{:}2,3\text{-}d])thiophene))]^+$ $[BF_4]^-$ (**5b**)*

Experimental procedures and work-up were as described in Section 4.3. Experimental details: **2b** (0.30 g, 0.13 mmol), [**1**]BF_4 (0.30 g, 0.07 mmol). Yield: 0.035 g, 65% based on [**1**]BF_4. Obtained as a dark purple solid. ^{1}H-NMR (500 MHz, CD_2Cl_2): δ 9.42 (d, 1H, *J* 12.7 Hz, μ-C–C*H*), 8.41 (s, 1H, Th), 8.01 (d, 1H, *J* 12.7 Hz, μ-C–CH=C*H*), 7.72 (d, 1H, *J* 4.9 Hz, Th), 7.38 (d, 1H, *J* 4.9 Hz, Th), 5.24 (s, 10H, C_5H_5). IR (CH_2Cl_2): 2033 (^{t}CO, 7), 1995 (^{t}CO, 2), 1841 (μ-CO, 3), 1605(8), 1526(10), 1384(3), 1223(9), 1182(4), 1139(3), 1113(2), 1057(2) cm^{-1}. IR (KBr disc): 2018 (^{t}CO, 8), 1982 (^{t}CO, 4), 1819 (μ-CO, 6), 1640(3), 1524(10), 1432(4), 1387(3.5), 1222(8) cm^{-1}. Anal. Calc. for $C_{24}H_{15}BF_4$-$Fe_2O_3S_3{\cdot}1.25CH_2Cl_2$: C, 40.27; H, 2.33. Found: C, 40.03; H, 2.32%. UV–Vis (CH_3CN): λ_{max} (ε) 545 (51250 M^{-1} cm^{-1}), 320 nm (10000 M^{-1} cm^{-1}). UV–Vis (CH_2Cl_2): λ_{max} (ε) 572 (65600 M^{-1} cm^{-1}), 330 nm (10000 M^{-1} cm^{-1}).

*4.3.3. $[Fe_2(\eta^5\text{-}C_5H_5)_2(CO)_2(\mu\text{-}CO)(\mu\text{-}(E)\text{-}C\text{–}CH{=}CH\text{-}2\text{-}(5\text{-}((E)\text{-}2\text{-}(2\text{-}thienyl)ethenyl)thiophene))]^+$ $[BF_4]^-$ (**5c**)*

Experimental procedures and work-up were as described in Section 4.3. Experimental details: **2c** (0.450 g, 2.0 mmol), [**1**]BF_4 (0.440 g, 1.0 mmol). Yield: 0.643 g, 97% based on [**1**]BF_4. Obtained as a dark blue solid. ^{1}H-NMR (500 MHz, CD_2Cl_2): δ 9.40 (d, 1H, J 13.7 Hz, μ-C–C*H*), 8.21 (d, 1H, *J* 3.4 Hz, Th), 7.92 (d, 1H, *J* 13.7 Hz, μ-C–CH=C*H*), 7.49 (d, 1H, *J* 16.1 Hz, Th–CH=C*H*–Th), 7.40 (d, 1H, *J* 4.9 Hz, Th), 7.28 (d, 1H, *J* 3.4 Hz, Th), 7.27 (d, 1H, *J* 16.1 Hz, Th–C*H*=CH–Th), 7.08 (m, 2H, Th), 5.29 (s, 10H, C_5H_5). ^{13}C-NMR (126 MHz, $CDCl_3$): δ 415.8 (μ-*C*), 255.9 (μ-*C*O), 207.5 (*C*O), 157.9, 149.6, 145.8, 141.7, 138.7, 130.5, 130.0, 128.8, 128.7, 128.0, 120.6, 91.7, 91.4. IR (CH_2Cl_2): 2031 (^{t}CO, 7), 2002 (^{t}CO, 2), 1841 (μ-CO, 4), 1561(1), 1532(10), 1516(5), 1491(2.5), 1379(3), 1212(6), 1181(5), 1112(2), 1046(3.5) cm^{-1}. IR (KBr disc): 2014 (^{t}CO, 9), 1976 (^{t}CO, 5.5), 1830 (μ-CO, 6), 1560(1), 1530(10), 1488(4), 1446(4.5), 1412(5), 1381(5), 1249(6), 1222(7), 1183(7), 1083(6), 1053(6), 949(2), 850(2), 519(2) cm^{-1}. Anal. Calc. for $C_{26}H_{19}BF_4Fe_2O_3S_2{\cdot}0.33CH_2Cl_2$: C, 47.35; H, 3.06. Found: C, 47.09; H, 3.01%. UV–Vis (CH_3CN): λ_{max} (ε) 575 (44750 M^{-1} cm^{-1}), 334 nm (15350 M^{-1} cm^{-1}). UV–Vis (CH_2Cl_2): λ_{max} (ε) 612 (36300 M^{-1} cm^{-1}), 339 nm (14950 M^{-1} cm^{-1}).

*4.3.4. $[Fe_2(\eta^5\text{-}C_5H_5)_2(CO)_2(\mu\text{-}CO)(\mu\text{-}(E)\text{-}C\text{–}CH{=}CH\text{-}7\text{-}(thieno[3,2\text{-}e][1]benzothiophene))]^+$ $[BF_4]^-$ (**5d**)*

Experimental procedures and work-up were as described in Section 4.3. Experimental details: **2d** (0.110 g, 0.5 mmol), [**1**]BF$_4$ (0.101 g, 0.23 mmol). Yield: 0.144 g, 95% based on [**1**]BF$_4$. Obtained as a dark red solid. ^{1}H-NMR (500 MHz, CD$_2$Cl$_2$): δ 9.62 (bs, 1H, μ-C–C*H*), 9.06 (s, 1H, Th), 8.23 (bs, 1H, μ-C–CH=C*H*), 8.10 (d, 1H, *J* 7.8 Hz, Ph), 8.02 (bs, 1H, Th), 7.87 (d, 1H, *J* 7.8 Hz, Ph), 7.81 (bs, 1H, Th), 5.37 (s, 10H, C$_5$*H*$_5$). ^{13}C-NMR (126 MHz, CDCl$_3$): δ 428.2 (μ-*C*), 254.3 (μ-*C*O), 207.7 (*C*O), 151.9, 147.2, 143.9, 140.2, 139.8, 138.4, 136.9, 136.6, 130.2, 125.1, 124.0, 119.2, 92.4. IR (CH$_2$Cl$_2$): 2035 (^{t}CO, 9), 2006 (^{t}CO, 2), 1842 (μ-CO, 4), 1537(9), 1522(10), 1254(1.5), 1166(8), 1061(2.5) cm^{-1}. IR (KBr disc): 2022 (^{t}CO, 9), 1992 (^{t}CO, 4), 1832 (μ-CO, 5), 1617(4), 1536(7), 1521(10), 1432(1), 1255(5), 1166(7), 1130(4.5), 1084(5) cm^{-1}. Anal. Calc. for $C_{26}H_{17}BF_4Fe_2O_3S_2 \cdot 0.25CH_2Cl_2$: C, 47.78; H, 2.64. Found: C, 47.76; H, 2.65%. UV–Vis (CH$_3$CN): λ_{max} (ε) 509 (46000 M^{-1} cm^{-1}), 318 nm (17650 M^{-1} cm^{-1}). UV–Vis (CH$_2$Cl$_2$): λ_{max} (ε) 538 (51550 M^{-1} cm^{-1}), 327 nm (13500 M^{-1} cm^{-1}). The structure was also established by X-ray analysis (Fig. 5).

*4.3.5. [Fe$_2$(η^5-C$_5$H$_5$)$_2$(CO)$_2$(μ-CO)(μ-(E)-C–CH=CH-2-(4,5,4′,5′-tetrahydro-[6,6′]bi[cyclopenta[b]thiophenylidene]))]$^+$ [BF$_4$]$^-$ (**5e**)*

Experimental procedures and work-up were as described in Section 4.3. Experimental details: **2e** (0.07 g, 0.26 mmol), [**1**]BF$_4$ (0.440 g, 0.1 mmol). Yield: 0.052 g, 73% based on [**1**]BF$_4$. Obtained as a dark blue–green solid. ^{1}H-NMR (500 MHz, CD$_2$Cl$_2$): δ 9.27 (b, 1H, μ-C–C*H*), 7.97 (m, 2H, μ-C–CH=C*H*, Th), 7.60 (d, 1H, *J* 4.9 Hz, Th), 6.98 (d, 1H, *J* 4.9 Hz, Th), 5.17 (s, 10H, C$_5$*H*$_5$). 3.0–3.4 (m, 8H, C*H*$_2$). ^{13}C-NMR (126 MHz, CDCl$_3$): δ 194.2 (μ-*C*), 257.9 (μ-*C*O), 208.7 (*C*O), 165.9, 159.1, 156.7, 147.6, 146.8, 144.9, 144.5, 143.3, 140.8, 136.9, 127.7, 124.6, 91.1, 38.3, 35.6, 28.7, 27.2. IR (CH$_2$Cl$_2$): 2024 (^{t}CO, 5), 1995 (^{t}CO, 1), 1834 (μ-CO, 3), 1604(5), 1526(7), 1390(2), 1215(10), 1140(6.5), 1112(3), 1062(2) cm^{-1}. IR (KBr disc): 2010 (^{t}CO, 6), 1980 (s, ^{t}CO, 4), 1821 (μ-CO, 4), 1598(1), 1518(8), 1422(5), 1395(6), 1286(3), 1198(10), 1136(8) cm^{-1}. Anal. Calc. for $C_{30}H_{23}BF_4Fe_2O_3S_2 \cdot 0.25CH_2Cl_2$: C, 50.89; H, 3.28. Found: C, 50.71; H, 3.26%. UV–Vis (CH$_3$CN): λ_{max} (ε) 680 (75900 M^{-1} cm^{-1}), 340 mn (15200 M^{-1} cm^{-1}). UV–Vis (CH$_2$Cl$_2$): λ_{max} (ε) 709 (105550 M^{-1} cm^{-1}), 347 nm (14200 M^{-1} cm^{-1}).

*4.3.6. [Fe$_2$(η^5-C$_5$H$_5$)$_2$(CO)$_2$(μ-CO)(μ-(E)-C–CH=CH-2-(5-(2-(5-((E)-2-ferrocenylethenyl)thienyl)thiophene)))] + [BF$_4$]$^-$ (**6a**)*

Experimental procedures and work-up were as described in Section 4.3. Experimental details: **4a** (0.080 g, 0.2 mmol), [**1**]BF$_4$ (0.070 g, 0.16 mmol). Yield: 0.098 g, 69% based on [**1**]BF$_4$. Obtained as a dark blue solid. ^{1}H-NMR (500 MHz, CD$_2$Cl$_2$): δ 9.27 (d, 1H, *J* 13.1 Hz, μ-C–C*H*), 8.18 (s, 1H, Th), 7.89 (d, 1H, *J* 13.6 Hz, μ-C–CH=C*H*), 7.37 (d, 1H, *J* 3.9 Hz, Th), 7.26 (d, 1H, *J* 3.4 Hz, Th), 6.86 (b, 1H, Th), 6.79 (d, 1H, *J* 15.6 Hz, Fc–CH=C*H*), 6.65 (d, 1H, *J* 15.6 Hz, Fc–C*H*=CH), 5.18 (s, 10H, C$_5$*H*$_5$), 4.53 (m, 2H, FcαH), 4.42 (m, 2H, FcβH), 4.18 (s, 5H, C$_5$*H*$_5$). ^{13}C-NMR (126 MHz, CDCl$_3$): δ 412.5 (μ-*C*), 255.9 (μ-*C*O), 208.2 (*C*O), 151.0,149.0, 144.8, 144.3, 141.7, 133.7, 127.3, 125.2, 123.4, 122.7, 119.1, 114.5, 88.3, 86.9, 66.3, 65.9, 63.4. IR (CH$_2$Cl$_2$): 2031 (^{t}CO, 10), 1996 (^{t}CO, 3), 1842 (μ-CO, 4), 1605(6), 1540(3), 1519(6), 1492(3), 1377(5), 1186(8), 1142(3), 1115(2), 1051(4) cm^{-1}. IR (KBr disc): 2019 (^{t}CO, 10), 1987 (^{t}CO, 5), 1830 (μ-CO, 6), 1636(1), 1518(9.5), 1430(8), 1376(5), 1258(4), 1186(9), 1145(6), 1049(6), 794(2) cm^{-1}. Anal. Calc. for $C_{36}H_{27}BF_4Fe_3O_3S_2 \cdot 0.75CH_2Cl_2$: C, 49.56; H, 3.15. Found: C, 49.85; H, 3.43%. UV–Vis (CH$_3$CN): λ_{max} (ε) 670 (15600 M^{-1} cm^{-1}), 577 (31600 M^{-1} cm^{-1}), 336 nm (20950 M^{-1} cm^{-1}). UV–Vis (CH$_2$Cl$_2$): λ_{max} (ε) 733 (10500 M^{-1} cm^{-1}), 606 (27400 M^{-1} cm^{-1}), 332 (14200 M^{-1} cm^{-1}).

*4.3.7. [Fe$_2$(η^5-C$_5$H$_5$)$_2$(CO)$_2$(μ-CO)(μ-(E)-C–CH=CH-3-(6-((E)-2-ferrocenylethenyl)dithieno-[3,2-b:2,3-d]-thiophene))]$^+$ [BF$_4$]$^-$ (**6b**)*

Experimental procedures and work-up were as described in Section 4.3. Experimental details: **4b** (0.070 g, 0.16 mmol), [**1**]BF$_4$ (0.040 g, 0.09 mmol). Yield: 0.66 g, 86% based on [**1**]BF$_4$. Obtained as a dark blue solid. ^{1}H-NMR (500 MHz, CD$_2$Cl$_2$): δ 9.40 (d, 1H, *J* 13.7 Hz, μ-C–C*H*), 8.43 (s, 1H, Th), 8.07 (d, 1H, *J* 13.7 Hz, μ-C–CH=C*H*), 7.16 (s, 1H, Th), 6.95 (d, 1H, *J* 16.1 Hz, Fc–C*H*=CH), 6.80 (d, 1H, *J* 16.1 Hz, Fc–CH=C*H*), 5.26 (s, 10H, C$_5$*H*$_5$), 4.67 (m, 2H, FcαH), 4.55 (m, 2H, FcβH), 4.27 (s, 5H, C$_5$*H*$_5$). ^{13}C-NMR (126 MHz, CD$_2$Cl$_2$): δ 409.6 (μ-*C*), 256.2 (μ-*C*O), 208.2 (*C*O), 153.3, 151.9, 149.0, 147.3, 146.0, 144.0, 140.6, 137.7, 133.5, 129.6, 119.8, 119.0, 93.2, 91.6, 71.7, 70.8, 68.6. IR (CH$_2$Cl$_2$): 2031 (^{t}CO, 5), 2000 (^{t}CO, 1), 1841 (μ-CO, 3), 1606(6), 1522(10), 1393(6), 1198(10), 1146(5), 1059(2) cm^{-1}. IR (KBr disc): 2019 (^{t}CO, 7), 1989 (^{t}CO, 4), 1830 (μ-CO, 4), 1637(7), 1617(10), 1522(8), 1384(4), 1201(7) cm^{-1}. Anal. Calc. for $C_{36}H_{25}BF_4Fe_3O_3S_3$: C, 50.5; H, 2.90. Found: C, 50.06; H, 3.14%. UV–Vis (CH$_3$CN): λ_{max} (ε) 680 (23400 M^{-1} cm^{-1}), 591 (36050 M^{-1} cm^{-1}), 356 nm (16200 M^{-1} cm^{-1}). UV–Vis (CH$_2$Cl$_2$): λ_{max} (ε) 747 (19400 M^{-1} cm^{-1}), 621 (343450 M^{-1} cm^{-1}), 333 nm (17350 M^{-1} cm^{-1}).

*4.3.8. [Fe$_2$(η^5-C$_5$H$_5$)$_2$(CO)$_2$(μ-CO)(μ-(E)-C–CH=CH-2-(5-((E)-2-(5-((E)-2-ferrocenylethenyl)-2-thienyl)-ethenyl)thiophene))]$^+$ [BF$_4$]$^-$ (**6c**)*

Experimental procedures and work-up were as described in Section 4.3. Experimental details: **4c** (0.060 g, 0.14 mmol), [**1**]BF$_4$ (0.040 g, 0.09 mmol). Yield: 0.57 g, 74% based on [**1**]BF$_4$. Obtained as a dark blue solid. ^{1}H-NMR (500 MHz, CD$_2$Cl$_2$): δ 9.36 (d, 1H, *J* 13.7 Hz, μ-C–C*H*), 8.21 (s, 1H, Th), 7.93 (d, 1H, *J* 13.7 Hz, μ-C–CH=C*H*), 7.43 (d, 1H, *J* 15.6 Hz, Th–C*H*=CH–Th), 7.24 (d, 1H, *J* 3.4 Hz, Th), 7.14 (d, 1H, *J* 3.4 Hz, Th), 6.99 (d, 1H, *J* 15.6 Hz, Th–CH=C*H*–Th), 6.89 (d, 1H, *J* 3.9 Hz, Th), 6.79 (d, 1H, *J* 16.1 Hz, Fc–C*H*=CH), 6.78 (d, 1H, *J* 16.1 Hz, Fc–CH=C*H*), 5.26 (s, 10H, C_5H_5), 4.50 (m, 2H, FcαH), 4.39 (m, 2H, FcβH), 4.19 (s, 5H, C_5H_5). ^{13}C-NMR (126 MHz, $CDCl_3$): δ 411.5 (μ-*C*), 256.6 (μ-*C*O), 207.6 (*C*O), 159.0, 149.4, 147.0, 146.2, 145.9, 139.5, 138.7, 132.1, 130.5, 130.5, 129.3, 126.5, 119.9, 119.3, 92.8, 91.3, 70.31, 70.0, 69.8. IR (CH_2Cl_2): 2030 (^{t}CO, 8), 2001 (^{t}CO, 2), 1839 (μ-CO, 4), 1605(1), 1587(2), 1530(10), 1517(7) cm^{-1}. IR (KBr disc): 2017 (^{t}CO, 7), 1998 (s, ^{t}CO, 4), 1828 (μ-CO, 5), 1518(10), 1412(7), 1384(5.5), 1217(8), 1179(8), 1106(7), 1084(6), 1044(7), 938(2), 833(1.5), 805(1.5) cm^{-1}. Anal. Calc. for $C_{38}H_{29}BF_4Fe_3O_3S_2$: C, 53.52; H, 3.40. Found: C, 54.05; H, 3.71%. UV–Vis (CH_3CN): λ_{max} (ε) 680 (35350 M^{-1} cm^{-1}), 648 (37350 M^{-1} cm^{-1}), 339 nm (16600 M^{-1} cm^{-1}). UV–Vis (CH_2Cl_2): λ_{max} (ε) 750 (31200 M^{-1} cm^{-1}), 669 (37750 M^{-1} cm^{-1}), 669 (33750 M^{-1} cm^{-1}), 339 nm (21550 M^{-1} cm^{-1}).

4.3.9. *[$Fe_2(\eta^5$-$C_5H_5)_2(CO)_2$(μ-CO)(μ-(E)-C–CH=CH-2-(7-((E)-2-ferrocenylethenyl)thieno-[3,2-e][1]-benzothiophene))]$^+$ [BF_4]$^-$* ***(6d)***

Experimental procedures and work-up were as described in Section 4.3. Experimental details: **4d** (0.050 g, 0.17 mmol), [**1**]BF_4 (0.040 g, 0.09 mmol). Yield: 0.051 g, 65% based on [**1**]BF_4. Obtained as a dark blue solid. ^{1}H-NMR (500 MHz, CD_2Cl_2): δ 9.46 (d, 1H, *J* 14.2 Hz, μ-C–C*H*), 8.90 (s, 1H, Th), 8.15 (d, 1H, *J* 13.7 Hz, μ-C–CH=C*H*), 7.88 (d, 1H, *J* 8.3 Hz, Ph),7.66 (d, 1H, *J* 8.3Hz, Ph), 7.56 (s, 1H, Th), 6.80 (s, 2H, Fc–C*H*=C*H*), 5.25 (s, 10H, C_5H_5), 4.74 (m, 2H, FcαH), 4.55 (m, 2H, FcβH), 4.29 (s, 5H, C_5H_5). ^{13}C-NMR (126 MHz, $CDCl_3$): δ 426.8 (μ-*C*), 254.8 (μ-*C*O), 207.8 (*C*O), 151.4, 147.2, 146.8, 143.6, 140.3, 139.9, 137.6, 137.0, 136.2, 132.1, 124.4, 121.5, 120.9, 119.4, 93.5, 92.0, 72.2, 72.0, 68.8. IR (CH_2Cl_2): 2036 (^{t}CO, 6), 2006 (^{t}CO, 1), 1844 (μ-CO, 3), 1606(4), 1537(4), 1520(10), 1383(2), 1351(1), 1330(1), 1156(2), 1138(2.5), 1113(4) cm^{-1}. IR (KBr disc): 2023 (^{t}CO, 7), 1994 (s, ^{t}CO, 4), 1832 (μ-CO, 5), 1522(10), 1431(1), 1330(4), 1254(5.5), 1191(4), 1162(6), 1138(6), 1084(7), 793(3), 724(2), 638(1) cm^{-1}. Anal. Calc. for $C_{38}H_{27}BF_4Fe_3O_3S_2\cdot0.33CH_2Cl_2$: C, 52.38; H, 3.15. Found: C, 52.38; H, 3.16%. UV–Vis (CH_3CN): λ_{max} (ε) 508 (29500 M^{-1} cm^{-1}), 346 nm (32350 M^{-1} cm^{-1}). UV–Vis (CH_2Cl_2): λ_{max} (ε) 630 (10600 M^{-1} cm^{-1}), 543 nm (35200 M^{-1} cm^{-1}), 341 nm (30650 M^{-1} cm^{-1}).

4.3.10. *[$Fe_2(\eta^5$-$C_5H_5)_2(CO)_2$(μ-CO)(μ-(E)-C–CH=CH-2-(2′-((E)-2-ferrocenylethenyl)-4,5,4′,5′-tetrahydro-[6,6′]-bi[cyclopenta[b]thiophenylidene]))]$^+$ [BF_4]$^-$* ***(6e)***

Experimental procedures and work-up were as described in Section 4.3. Experimental details: **4e** (0.080 g, 0.17 mmol), [**1**]BF_4 (0.040 g, 0.09 mmol). Yield: 0.51 g, 58% based on [**1**]BF_4. Obtained as a dark green solid. ^{1}H-NMR (500 MHz, CD_2Cl_2): δ 9.1–9.2 (vbs, 1H, μ-C–C*H*), 7.6–8.0 (bm, 2H, μ-C–CH=C*H*, Th), 6.8–7.0 (bm, 3H, Fc–C*H*=C*H*, Th), 5.2 (10H, bs, C_5H_5), 4.0–4.4 (bm, 9H, Fc), 3.0–3.4 (bm, 8H, C*H*$_2$). ^{13}C-NMR (126 MHz, $CDCl_3$): δ 385.3 (μ-*C*), 258.9 (μ-*C*O), 209.0 (*C*O), 166.6, 162.0, 161.2, 157.2, 147.2, 145.6, 145.1, 144.5, 142.9, 140.1, 131.6, 128.2, 122.2, 120.5, 92.6, 90.9, 71.5, 70.9, 68.2, 38.0, 35.7, 28.8, 27.1. IR (CH_2Cl_2): 2032 (^{t}CO, 7), 1995 (^{t}CO, 2), 1833 (μ-CO, 4), 1601(8), 1580(6), 1526(7), 1460(10), 1379(9), 1194(7) cm^{-1}. IR (KBr disc): 2010 (^{t}CO, 8), 1975 (s, ^{t}CO, 5), 1821 (μ-CO, 5), 1637(7), 1618(10), 1420(4), 1379(4), 1211(9.5), 1137(7), 1084(7) cm^{-1}. Anal. Calc. for $C_{42}H_{33}BF_4Fe_3O_3S_2\cdot0.5CH_2Cl_2$: C, 53.88; H, 3.59. Found: C, 53.73; H, 3.65%. UV–Vis (CH_3CN): λ_{max} (ε) 769 (40900 M^{-1} cm^{-1}), 700 (37800 M^{-1} cm^{-1}), 340 nm (15950 M^{-1} cm^{-1}). UV–Vis (CH_2Cl_2): λ_{max} (ε) 830 (41850 M^{-1} cm^{-1}), 716 (40100 M^{-1} cm^{-1}), 340 (17400 M^{-1} cm^{-1}).

Table 3
Crystal data and structure refinement for [**5d**]BF_4

Compound	[**5d**]$BF_4\cdot CH_2Cl_2$
Empirical formula	$C_{27}H_{19}BCl_2F_4Fe_2O_3S_2$ $[C_{26}H_{17}Fe_2O_3S_2]^+[BF_4]^-\cdot CH_2Cl_2$
Formula weight	724.95
Temperature (K)	296(2)
Wavelength (Å)	0.70930
Crystal system, space group	Triclinic, $P\bar{1}$
Unit cell dimensions	
a (Å)	10.934(2)
b (Å)	12.419(2)
c (Å)	13.356(2)
α (°)	117.383(7)
β (°)	93.943(10)
γ (°)	107.550(9)
Volume (Å^3)	1488.6(4)
Z	2
Calculated density (Mg m^{-3})	1.617
Absorption coefficient (mm^{-1})	1.348
F(000)	728
Crystal size (mm)	0.17 × 0.15 × 0.13
θ range for data collection (°)	1.88–25.5
Index ranges	*h* −13–13, *k* −13–13, *l* 0–16
Reflections collected/unique	5124/5124 [$R_{int}=0.00$]
Completeness to $2\sigma = 25.0$ (%)	99.0
Max. and min. transmission	0.85, 0.80
Refinement method	Full-matrix least-squares on F^2
Data/restraints/parameters	5124/92/444
Goodness-of-fit on F^2	1.013
Final *R* indices [$I > 2\sigma(I)$]	$R_1 = 0.0601$, $wR_2 = 0.0997$
R indices (all data)	$R_1 = 0.1464$, $wR_2 = 0.1277$
Largest difference peak and hole (e Å^{-3})	0.29 and −0.26

4.4. X-ray data collection

A single crystal of [**5d**]BF_4^- was grown from diethyl ether–dichloromethane. Details of the X-ray data collection and structural refinement are summarised in Table 3. The structure was solved using direct methods in SHELXS97 [29] and refined by full-matrix least-squares techniques using SHELXL97 [30]. The hydrogen atoms were treated as riding atoms with C–H distances in the range 0.93–0.98 Å [SHELXL97 defaults]. It was evident during the penultimate stages of refinement (when R [$F^2 > 2\sigma(F^2)$] was 0.09) that there were minor components of disorder associated with the $[BF_4]^-$ anion and the dichloromethane solvent molecule. Coordinates for the minor sites of the anion and solvent were generated and, for the final refinement cycles, soft DFIX and DELU/ISOR restraints were used in the SHELXL97 calculations [30]. The atoms of the major and minor conformations of the $[BF_4]^-$ anion and solvent were refined with anisotropic displacement parameters to final site occupancies of 0.827(12)/0.173(12) and 0.530(8)/0.470(8) respectively; disorder in a $[BF_4]^-$ anion is relatively common [31]. The final R-factor is 0.060 for 2595 observed reflections [$I > 2\sigma(I)$] out of a total of 5124 measured reflections.

5. Supplementary material

Crystallographic data for the structural analysis have been deposited with the Cambridge Crystalographic Data Centre, CCDC no. 145941 for compound [**5d**]BF_4. Copies of this information may be obtained free of charge from The Director, CCDC, 12 Union Road Cambridge, CB2 1EZ, UK (Fax: +44-1223-336033; e-mail: deposit@ccdc.cam.ac.uk or www: http://www.ccdc.cam.ac.uk).

Acknowledgements

This work was supported by the EU under the TMR network CT-98-0166. We also acknowledge the support of the Belgian Government (IUAP IV/11), the Fund for Scientific Research-Flanders (FWO G.0338.98; 9.0407.98) and the University of Leuven (GOA 2000/03). J.F.G. thanks Dublin City University for the purchase of a Bruker AXS P4 diffractometer. Elemental analyses were performed by Ms A. Connolly and many thanks are due to Dr Natalie Cromhout for helpful discussions during the preparation of this manuscript.

References

[1] (a) N.J. Long, Angew. Chem. Int. Ed. Engl. 34 (1995) 21. (b) T. Verbiest, S. Houbrechts, M. Kauranen, K. Clays, A. Persoons, J. Mater. Chem. 7 (1997) 2175. (c) I.R. Whittall, A.M. McDonagh, M.G. Humphrey, Adv. Organomet. Chem. 42 (1998) 291. (d) J. Heck, S. Dabek, T. Meyer-Friedrichsen, H. Wong, Coord. Chem. Rev. (1999) 1217.

[2] D.N. Prasad, D.J. Williams, Introduction to Nonlinear Optical Effects in Molecules and Polymers, Wiley, New York, 1991.

[3] M. Nitay, W. Priester, M. Rosenblum, J. Am. Chem. Soc. 100 (1978) 3620.

[4] J.A. Bandy, H.E. Bunting, M.-H. Garcia, M.L. Green, S.R. Marder, M.E. Thompson, D. Bloor, P.V. Kolinsky, R.J. Jones, J.W. Perry, Polyhedron 11 (1992) 1429.

[5] C.P. Casey, M.S. Konings, S.R. Marder, Y. Takezawa, J. Organomet. Chem. 358 (1988) 347.

[6] (a) C.P. Casey, M.S. Konings, R.E. Palermo, R.E. Colborn, J. Am. Chem. Soc. 107 (1985) 5296. (b) C.P. Casey, M.S. Konings, S.R. Marder, J. Organomet. Chem. 345 (1988) 125.

[7] T. Farrel, T. Meyer-Friedrichsen, J. Heck, A.R. Manning, Organometallics 19 (2000) 3410.

[8] (a) J. Roncali, Annu. Rep. Prog. Chem. Sect. C 95. (1999) 47. (b) J. Roncali, Chem. Rev. 97 (1997) 173 and refs. cited therein.

[9] H. Wynberg, A. Logothetis, J. Am. Chem. Soc. 78 (1956) 1958.

[10] F. De Jong, M.J. Jansen, J. Org. Chem. 36 (1971) 1645.

[11] J. Nakayama, T. Fujimori, Heterocycles 32 (1991) 991.

[12] R.M. Kellog, M.B. Groen, H. Wynberg, J. Org. Chem. 32 (1967) 3093.

[13] J. Roncali, C.T. Gautier, E.H. Elandaloussi, P. Frére, J. Chem. Soc. Chem. Commun. (1994) 2249.

[14] (a) R. Antonioletti, M. D'Auria, F. D'Onofrio, G.A. Piancatelli, A. Scettri, J. Chem. Soc. Perkin Trans. 1 (1986) 1755. (b) US Patent Appl. (1992) 930732 [Chem. Abstr. 122 (1993) P241800]. (c) See ref. [10]. (d) M.B. Groen, H. Schadenberg, H. Wynberg, J. Org. Chem. 36 (1971) 2792.

[15] (a) R.F. Curtis, G.T. Phillips, Tetrahedron 23 (1967) 4419. (b) O.-K. Kim, J.-M. Lehn, Chem. Phys. Lett. 255 (1996) 147. (c) J.X. Zhang, P. Dubois, R. Jêrome, J. Chem. Soc. Perkin Trans. 2 (1997) 1209. (d) See ref. [14d].

[16] (a) P.L. Pauson, W.E. Watts, J. Chem. Soc. (1963) 2990. (b) H.E. Baumgarten (Ed.), Org. Synth. Col. vol. V, Wiley, New York, 1973, p. 434.

[17] A. Berlin, S. Bradamante, R. Ferraccioli, G.A. Pagani, F. Sannicolò, J. Chem. Soc. Perkin Trans. 1 (1987) 2631.

[18] V.P. Rao, A.K.-Y. Jen, K.Y. Wang, K.J. Drost, J. Chem. Soc. Chem. Commun. (1993) 1118.

[19] (a) F. Effenberger, F. Würthner, Angew. Chem. Int. Ed. Engl. 32 (1993) 719. (b) S.L. Gilat, S.H. Kawai, J.-M. Lehn, J. Chem. Soc. Chem. Commun. (1993) 1439. (c) S.L. Gilat, S.H. Kawai, J.-M. Lehn, Chem. Eur. J. 1 (1995) 275.

[20] K.N. Jayaprakash, P.C. Ray, I. Matsuoka, M.M. Bhadbhade, V.G. Puranik, P.K. Das, H. Nishihara, A. Sarkar, Organometallics 18 (1999) 3851.

[21] P. McArdle, J. Appl. Crystallogr. 28 (1995) 65.

[22] S.R. Marder, C.B. Gorman, F. Meyers, J.W. Perry, G. Bourhill, J.-L. Brédas, B.M. Pierce, Science 265 (1994) 632.

[23] J. March, Advanced Organic Chemistry, Wiley, New York, 4th Ed., 1992.

[24] (a) K. Clays, A. Persoons, Phys. Rev. Lett. 66 (1991) 2980. (b) K. Clays, A. Persoons, Rev. Sci. Instrum. 6 (1992) 3285.

[25] (a) N. Bloembergen, Y.R. Shen, Phys. Rev. 133 (1964) 37. (b) J.L. Oudar, D.S. Chemla, J. Chem. Phys. 66 (1976) 2664.

[26] S.M. LeCours, H.W. Guan, S.G. DiMangno, C.H. Wang, M.J. Therien, J. Am. Chem. Soc. 118 (1996) 1495.

[27] (a) I.R. Whittall, A.M. McDonagh, M.G. Humphrey, M. Samoc, Adv. Organomet. Chem. 42 (1998) 291. (b) B.J. Coe, S. Houbrechts, I. Asselberghs, A. Persoons, Angew. Chem. Int. Ed. Engl. 38 (1999) 366. (c) G.G.A. Balavoine, J.C. Daran, G. Iftime, P.G. Lacroix, E. Manoury, J.A. Delaine, I. Maltey-Fanton, K. Nakatani, S.D. Bella, Organometallics 18 (1999) 21. (d) I.S. Lee, H. Seo, Y.K. Chung, Organometallics 18 (1999) 1091.

[28] T.L. Gilchrist, Heterocyclic Chemistry, Wiley, New York 1985.

[29] G.M. Sheldrick, SHELXS97, Program for the Solution of Crystal Structures, University of Göttingen, Germany, 1997.

[30] G.M. Sheldrick, SHELXL97, Program for the Refinement of Crystal Structures, University of Göttingen, Germany, 1997.

[31] J.F. Gallagher, E.C. Alyea, G. Ferguson, X. Zheng, Acta Crystallogr. Sect. C 50 (1994) 16.